2020 17th International Conference on Electrical Engineering, Computing Science and Automatic Control (CCE), Mexico City, Mexico. November 11-13, 2020

Visual Object Tracking with Colored Measurement Noise using Kalman and UFIR Filters

Yuriy S. Shmaliy, José Andrade-Lucio,
Eli G. Pale-Ramon, Jorge Ortega-Contreras
Electronics Engineering Dept.
Universidad de Guanajuato
Salamanca, Gto., Mexico
eligpale@gmail.com, {shmaliy, andrade, ja.ortegacontreras} @ugto.mx

Luis J. Morales-Mendoza, Mario González-Lee
Electronics Engineering Dept.
Universidad Veracruzana
Poza Rica, Ver., Mexico
{javmorales, mgonzalez01} @uv.mx

***Abstract*—Visual object tracking is commonly accompanied with large variations in the image frame size and position, as caused by the object dynamics and low frame rate. In this paper, we treat such variations as a Gauss-Markov colored measurement noise (CMN), modify the Kalman filter and unbiased finite impulse response filter using the backward Euler method and employing measurement differencing, and apply to some simulated and benchmark data. It is shown that the modified filters can suppress efficiently both the slow frame variations associated with CMN and fast variations associated with white noise. Extensive experimental investigations conducted for the "Car4" benchmark database has demonstrated a high efficiency of the modified algorithms.**

***Index Terms*—Visual object tracking, colored measurement noise, Kalman filter, unbiased FIR filter**

I. Introduction

Visual object tracking is a well-recognized problem of estimating the trajectory of some target over a sequence of images across frames [1]. As such, it is fundamental in computer vision, but also establishes a steady topis for signal and image processing [2]–[4], where coordinates of a sequence of frames are considered as data for the object trajectory estimation.

When a video camera catches an object and then track it in time, consecutive video frames do not follow an object exactly, especially when an object moves faster than the frame rate [5], that is akin to problems in bandlimited channels [6] and narrowband receivers [7]. A similar effect is viewed when an object changes orientation over time. An efficient way to avoid large tracking errors is to employ a motion model and use state estimators [8]–[16]. If the model is carefully specified in state space, it may represent the object dynamics for different possible motions quite accurately. But, even so, the tracking accuracy will still highly dependent on the measurement residuals representing data noise and mismodeling errors.

An example of possible frame appearances while catching a moving car is shown in Fig. 1 for the "Car2" benchmark [17], where a desirable (ideal) frame is shown in white. Since the frame coordinates vary with time, the variations can be considered as a colored measurement noise (CMN), which is not white [9], [18]. An estimator is thus desirable such that the CMN induced by the frame dynamics is filtered out optimally [19]–[26].

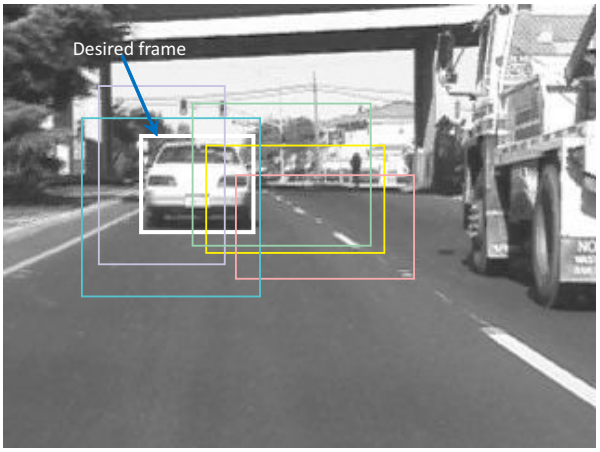

Fig. 1. Possible appearances of the video camera image frame in visual object tracking due to the object dynamics and low frame rate. A desirable frame is white.

Although, in the literature, there are various algorithms for tracking objects such as Circulant Structure Kernel (CSK), Vehicle Tracking Device (VTD), Structured Output Tracking with Kernels (Struck), among others [17]. In this paper, we use a modified Kalman filter (KF) and unbiased finite impulse response (UFIR). One of the reasons for using these methods is that they have been proven to reduce CMN with favorable results [9]. Likewise, the Kalman Filter has been used by various researchers as a method for tracking objects [27]–[30]. We view the image frame variations as CMN, modify the Kalman filter (KF) and unbiased finite impulse response (UFIR) filter for CMN using measurement differencing, provide simulations, investigate filtering errors, and apply the algorithms designed to benchmark data obtained from visual object tracking of a moving car. Based on the simulation and experimental testing, it is shown that the algorithms modified for CMN produce much smaller errors than the original algorithms.

This investigation was supported by the Mexican CONACyT-SEP Project A1-S-10287, Funding CB2017-2018.

978-1-7281-8987-1/20/$31.00 ©2020 IEEE

II. State-Space Model of a Moving Object with CMN Employing Measurement Differencing

The measurement differencing approach was proposed by Bryson in [31], [32] and results in the *Bryson algorithm* to make noise white via smoothing and filtering. In another *Petovello algorithm* [33], noise becomes white in one phase (filtering). Both these and other known modifications for CMN employ the prediction state-space model obtained by the forward Euler method. Because prediction is not required for our purposes, we used another state-space model produced by the backward Euler method:

$$\begin{aligned} x_n &= F_n x_{n-1} + B_n w_n \,, && (1)\\ v_n &= \Psi_n v_{n-1} + \xi_n \,, && (2)\\ y_n &= H_n x_n + v_n \,, && (3) \end{aligned}$$

where $x_n \in \mathbb{R}^K$ is the state vector, $y_n \in \mathbb{R}^M$ is the observation vector, $v_n \in \mathbb{R}^M$ is the Gauss-Markov CMN, and matrices $F_n \in \mathbb{R}^{K\times K}$, $B_n \in \mathbb{R}^{K\times P}$, $H_n \in \mathbb{R}^{M\times K}$, and $\Psi_n \in \mathbb{R}^{M\times M}$ are known and can be constant. Matrix Ψ_n is chosen such that the CMN v_n is stationary. Noise vectors $w_n \sim \mathcal{N}(0, Q_n) \in \mathbb{R}^P$ and $\xi_n \sim \mathcal{N}(0, R_n) \in \mathbb{R}^M$ are zero mean, $E\{w_n\} = 0$ and $E\{\xi_n\} = 0$, and white Gaussian with the covariances $E\{w_n w_k^T\} = Q_n\delta_{n-k}$ and $E\{\xi_n\xi_k^T\} = R_n\delta_{n-k}$ and the property $E\{w_n\xi_k^T\} = 0$ for all n and k.

A. Measurement Differencing for CMN

To avoid state augmentation, which makes the KF ill-conditioned [32], and CMN v_n in y_n, a new observation z_n is considered as a measurement difference, write

$$\begin{aligned} z_n &= y_n - \Psi_n y_{n-1} \,, \\ &= H_n x_n + v_n - \Psi_n H_{n-1} x_{n-1} - \Psi_n v_{n-1} \,, \quad (4) \end{aligned}$$

take x_{n-1} and v_{n-1} from (1), obtain

$$z_n = D_n x_n + \bar{v}_n \,, \quad (5)$$

where $D_n = H_n - \Gamma_n$, $\Gamma_n = \Psi_n H_{n-1} F_n^{-1}$, and $\bar{v}_n = \Gamma_n B_n w_n + \xi_n$ and notice that noise $\bar{v}_n$ is white with the properties

$$\begin{aligned} \bar{R}_n = E\{\bar{v}_n \bar{v}_n^T\} &= \Gamma_n \Phi_n + R_n \,, && (6)\\ E\{\bar{v}_n w_n^T\} &= \Gamma_n B_n Q_n \,, && (7) \end{aligned}$$

where $\Phi_n = B_n Q_n B_n^T \Gamma_n^T$. The modified model (1) and (5) has thus white and time-correlated w_n and $\bar{v}_n$.

B. Kalman Algorithm for CMN

Based on the backward Euler-based model (1)–(3) with CMN, the KF has been recently modified via measurement differences (5)in [9]. The modification results in two available KF algorithms for correlated and de-correlated noise sources. Also, it was shown that the algorithms have now an advantage against one another. Therefore, we employed the one derived for the de-correlated noise sources.

To de-correlate w_n and $\bar{v}_n$, one can refer to [34] and combine x_n taken from (1) with a term $\Lambda_n(z_n - D_n x_n - \bar{v}_n)$, where z_n is a data vector and Λ_n must be determined,

$$\begin{aligned} x_n &= F_n x_{n-1} + B_n w_n + \Lambda_n(z_n - D_n x_n - \bar{v}_n) \\ &= A_n x_{n-1} + u_n + \zeta_n \,, \quad (8) \end{aligned}$$

where $A_n = (I - \Lambda_n D_n)F_n$, $u_n = \Lambda_n z_n$, $\zeta_n = (I - \Lambda_n D_n)B_n w_n - \Lambda_n \bar{v}_n$, and noise $\zeta_n \sim \mathcal{N}(0, \mathcal{Q}_n) \in \mathbb{R}^K$ has the covariance $\mathcal{Q}_n = E\{\zeta_n \zeta_n^T\}$,

$$\mathcal{Q}_n = (I - \Lambda_n H_n) B_n Q_n B_n^T (I - \Lambda_n H_n)^T + \Lambda_n R_n \Lambda_n^T \,. \quad (9)$$

Matrix Λ_n making ζ_n and $\bar{v}_n$ uncorrelated can be found by transforming the desired property $E\{\zeta_n \bar{v}_n^T\} = 0$ that yields

$$\Lambda_n = \Phi_n (H_n \Phi_n + R_n)^{-1} \quad (10)$$

and allows finding

$$\mathcal{Q}_n = (I - \Lambda_n H_n) B_n Q_n B_n^T (I - \Lambda_n D_n)^T \,. \quad (11)$$

Provided the transformations, the KF modified for CMN with de-correlated noise sources is represented with a pseudocode listed as Algorithm 1 [9].As can be seen, Algorithm 1 requires a modified system noise covariance $\mathcal{Q}_n$ (11) and input $u_n = \Lambda_n z_n$ with Λ_n given by (10). It can easily be shown that $\Psi_n = 0$ makes this algorithm the standard KF.

Algorithm 1: KF for CMN with De-correlated w_n and $\bar{v}_n$

Data: y_n, $\hat{x}_0$, P_0, $\mathcal{Q}_n$, R_n
Result: $\hat{\mathbf{x}}_n$, P_n

begin
  for $n = 1, 2, \cdots$ **do**
    $D_n = H_n - \Psi_n H_{n-1} F_n^{-1}$
    $z_n = y_n - \Psi_n y_{n-1}$
    $\bar{P}_n^- = A_n P_{n-1} A_n^T + \mathcal{Q}_n$
    $\bar{S}_n = D_n \bar{P}_n^- D_n^T + \Gamma_n \Phi_n + R_n$
    $\bar{K}_n = \bar{P}_n^- D_n^T \bar{S}_n^{-1}$
    $\hat{\bar{x}}_n^- = A_n \hat{x}_{n-1} + \Lambda_n z_n$
    $\hat{x}_n = \hat{\bar{x}}_n^- + \bar{K}_n(z_n - D_n \hat{\bar{x}}_n^-)$
    $P_n = (I - \bar{K}_n D_n)\bar{P}_n^-$
  end for
end

C. UFIR Filter for CMN

The UFIR filter [35] [36] does not require any information about noise, except for the zero-mean assumption. That can be more suitable for visual object tracking, where neither the object noise nor the measurement noise is known exactly. However, it requires an optimal averaging horizon $[m, n]$ of $N_{\rm opt}$ points, from $m = n - N_{\rm opt} + 1$ to n, to minimize the MSE. Therefore, the UFIR filter cannot ignore the CMN v_n on short horizons.

A pseudocode of the UFIR filtering algorithm for CMN is listed as Algorithm 2. To avoid singularities, the algorithm

requires a short measurement vector $Y_{m,s} = [\, y_m \ \dots \ y_s \,]^T$ and matrix

$$C_{m,s} = \begin{bmatrix} D_m(F_s ... F_{m+1})^{-1} \\ \vdots \\ D_{s-1}F_s^{-1} \\ D_s \end{bmatrix}.$$

Note that $C_{m,s}^T C_{m,s}$ is singular if $s-m < K-1$ and thus the generalized noise power gain (GNPG) $G_s = (C_{m,s}^T C_{m,s})^{-1}$ cannot be computed on horizons shorter than K points. It also follows that, by $\Psi_n = 0$, Algorithm 2 becomes the standard UFIR filter [35].

Algorithm 2: UFIR Filter for Backward Euler Model with CMN

Data: N, y_n
Result: $\hat{x}_n$
begin
  for $n = N-1, N, \cdots$ **do**
    $m = n - N + 1$, $s = n - N + K$
    $G_s = (C_{m,s}^T C_{m,s})^{-1}$
    $\bar{x}_s = G_s C_{m,s}^T Y_{m,s}$
    for $l = s+1 : n$ **do**
      $D_l = H_l - \Psi_l H_{l-1} F_l^{-1}$
      $z_l = y_l - \Psi_l y_{l-1}$
      $G_l = [D_l^T D_l + (F_l G_{l-1} F_l^T)^{-1}]^{-1}$
      $K_l = G_l D_l^T$
      $\bar{x}_l^- = F_l \bar{x}_{l-1}$
      $\bar{x}_l = \bar{x}_l^- + K_l(z_l - D_l \bar{x}_l^-)$
    end for
    $\hat{x}_n = \bar{x}_n$
  end for
end

D. Simulation of Two-State Tracking under CMN

We now consider a two-state tracking problem and supposed that an object is disturbed by white Gaussian acceleration noise with the standard deviation of $\sigma_w = 50\,\mathrm{m/s^2}$. The CMN originates from white Gaussian ξ_n with $\sigma_\xi = 4\,\mathrm{m}$. A trajectory is simulated at 2000 points for $x_0 = [\, 1 \ 1 \,]^T$, $P_0 = 0$, $Q = \sigma_w^2$, $R = \sigma_v^2$, and

$$F = \begin{bmatrix} 1 & \tau \\ 0 & 1 \end{bmatrix}, \ B = \begin{bmatrix} \frac{\tau^2}{2} \\ \tau \end{bmatrix}, \ H = \begin{bmatrix} 1 & 0 \end{bmatrix}.$$

Following [37], we determine $N_{\mathrm{opt}} = \sqrt{\frac{12\sigma_\xi}{\tau^2 \sigma_w}} \cong 20$ for white noise and then update it experimentally for each ψ at a test stage. We reveal experimentally that N_{opt} changes linearly from 20 to 30 when ψ rises up to 0.6 and grows nonlinearly to reach 100 when $\psi = 0.95$. Function $N_{\mathrm{opt}}(\psi)$ measured in such a way is used in the UFIR algorithm.

Typical root MSEs (RMSEs) produced by the KF and UFIR algorithms as functions of ψ and averaged over multiple Monte Carlo (MC) runs are sketched in Fig. 2. In the case of Fig. 2a, we suppose that the noise statistics are known exactly. In another case of Fig. 2b, we assume that information about noise in incomplete and introduces the error factors $\{p, q\} > 0$ as $p^2 Q$ and $q^2 R$ in the algorithms.

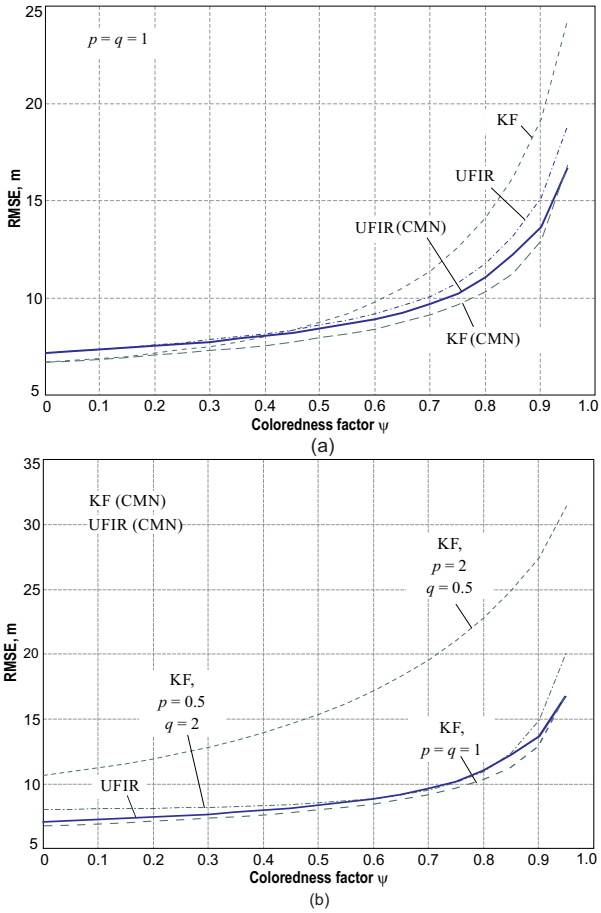

Fig. 2. Typical RMSEs produced by the modified KF and UFIR filter ($N_{\mathrm{opt}} = 20$) as functions of the coloredness factor ψ for the two-state tracking model under: (a) ideal conditions, $p = q = 1$, and (b) errors in the noise statistics, $p \neq 1$ and $q \neq 1$.

The following observations can be made by analysing this figure:

- Under the ideal conditions $p = q = 1$ (Fig. 2a), the KF is more sensitive to the coloredness factor ψ than the UFIR filter. However, the modified KF improves the performance more efficiently and produces smaller errors than the modified UFIR filter.
- Errors in the standard and modified UFIR filters do not get away essentially from one another. That means that the modified UFIR filter is more robust than the modified KF against the CMN.
- Errors in the noise statistics make the modified KF much less accurate even under small error factors $p = 0.5, q = 2$ and $p = 2, q = 0.5$ (Fig. 2b).

An overall conclusion, which is suggested by simulations is that the UFIR filter is more suitable for solving the tracking problem under errors in the noise statistics in the presence

of the CMN. Referring to the above, we now go on with experimental testing of visual object tracking algorithms.

III. Visual Tracking of a Moving Object

Visual object tracking has been organized based on the benchmark trajectory "Car4," which coordinates, and car frames are measured by the following car using a visual tracking system [17] with data are available from [38]. For visual tracking, this benchmark trajectory is one of the most used tracking sequences [17] due to it has a list of annotated attributes: illumination variation and scale variation. In this sequence, a car moves and maneuvers smoothly on a road in an urban area, although the car frames undergo rapid changes. To test filters by this trajectory, the measurements made are processed along coordinate x as shown in Fig. 3 in grey.

A comparison with the car actual trajectory shows that data have brightly pronounced CMN mostly caused the camera tracking ability (low frame rate).

The problem can be seen in Fig. 3a: as long as the car moves smoothly, fast variations should be removed from data. Because noise in data is not white, we suppose that it has a Gauss-Markov origin and consider it as CMN. Next, the filters are tuned for the above-discussed two-state model and test them by this trajectory. Since no additional information is provided in [38], we conduct filter tuning under some general assumptions.

The typical capturing rate of cameras for a low frame rate is 30 frames per second [39], [40]. Considering the trade off between the image quality and data transmission speed, we set the capturing rate to 20 frames per second or $\tau = 0.05\,\mathrm{s}$. We also suppose that the car acceleration noise is not large, set $\sigma_w = 3\,\mathrm{m/s^2}$, and accept $\sigma_\xi = 2\,\mathrm{m}$ for the data noise. Next, both values are examined experimentally for the standard KF to provide visually best denoising with no essential bias. It is seen in Fig. 3a that the standard KF tuned in such a way follows the slow (colored) parts of the trajectory and do not remove them, as required. To tune the UFIR filter, we find $N \cong 65$ for its output to range close to the standard KF and arrive at almost the same estimates as by the standard KF. A conclusion is thus that the standards filters are not suitable for visual object tracking (Fig. 3a).

We finally run the modified KF and realize experimentally that factor $\psi \cong 0.9$ fits with the data noise, allowing for best denoising. A subsequent minimization of the difference between the UFIR and KF outputs gave $N \cong 160$ and we set it to the modified UFIR algorithm. The results sketched in Fig. 3b has appeared to be quite impressive. In fact, the modified filters remove the colored noise from data very efficiently and the filtered trajectory traces much closer to the actual one. Another important conclusion arises from a comparison of the filter outputs. It follows that the difference between the KF and UFIR estimates is poorly distinguishable (Fig. 2) to mean that the UFIR filter, which does not require the noise statistics, is a better estimator for visual object tracking than the KF.

A complete picture of visual object tracking and estimation in the x-y plane is given in Fig. 4. Because the CMN is

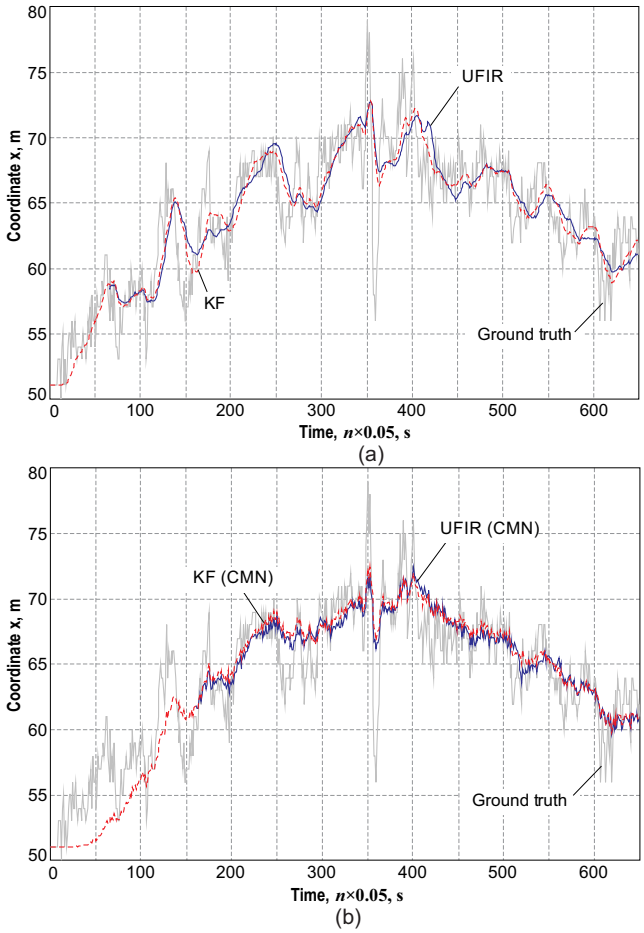

Fig. 3. A benchmark trajectory of a moving car ("Car4") along coordinate x and it estimation using: (a) standard KF and UFIR filter ($N = 65$) and (b) modified KF and UFIR filter with $N = 160$.

removed from both scales, we observe here several important effects. After tuned properly, both estimators behave quite similarly. However, the UFIR filter does not require information about noise and is thus more suitable for applications. All slow variations are efficiently filtered out so that the estimated trajectory looks much smoother and closer to the actual one. Although both estimators also filter out the fast noise components, a small amount of fast variations remains. On other hand, we consider that the current limitation of the proposed methods is that only were tested in the tracking of a single objective.

IV. Conclusions

The KF and UFIR estimation algorithms developed for CMN using measurement differencing have appeared to be highly efficient for visual object tracking in a sequence with annotated attributes (illumination variation and scale variation). An advantage is that slow frame variations associated with CMN are suppressed along with fast variations associated with white noise. That allows tracking moving objects more precisely. Simulations conducted for the two-state tracking problem have confirmed the theoretical inferences. Extensive

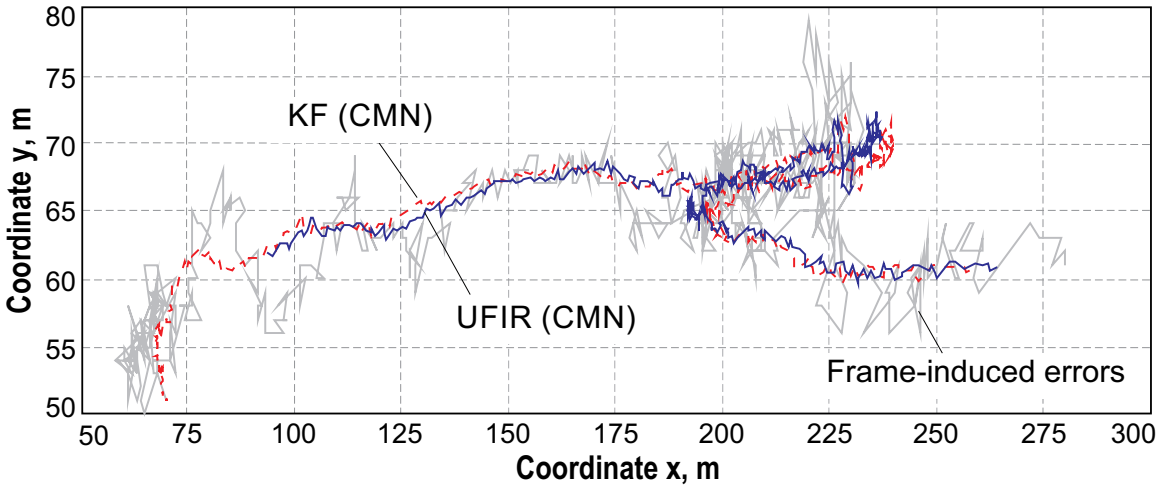

Fig. 4. Suppressing the frame slow variations associated with CMN and fast variations associated with white noise in x-y plane of the "Car4" benchmark using modified KF and UFIR filter.

experimental testing of visual object tracking based on the "Car4" benchmark contaminated by intensive CMN has fitted well with the simulation results. We thus conclude that further development of visual object tracking algorithms can be provided by incorporating the state estimators modified for CMN for a broad area of applications.

Referring to the high accuracy of the KF and UFIR filter developed in removing the CMN, we now design practical algorithms for video target tracking. In future works, the performance of these algorithms will be measured against conventional algorithms as well as emerging methods such as convolutional neural networks.

REFERENCES

[1] M. Danelljan, *Learning Convolution Operators for Visual Tracking*. Linköping University Electronic Press, 2018.

[2] A. N. Bishop, A. V. Savkin, and P. N. Pathirana, "Vision-based target tracking and surveillance with robust set-valued state estimation," *IEEE Signal Processing Letters*, vol. 17, no. 3, pp. 289–292, 2010.

[3] X. Zhou, Y. Li, B. He, and T. Bai, "GM-PHD-based multi-target visual tracking using entropy distribution and game theory," *IEEE Transactions on Industrial Informatics*, vol. 10, no. 2, pp. 1064–1076, 2014.

[4] Y. Yi and H. Xu, "Hierarchical data association framework with occlusion handling for multiple targets tracking," *IEEE Signal Processing Letters*, vol. 21, no. 3, pp. 288–291, 2014.

[5] M. Chuang, J. Hwang, K. Williams, and R. Towler, "Tracking live fish from low-contrast and low-frame-rate stereo videos," *IEEE Transactions on Circuits and Systems for Video Technology*, vol. 25, no. 1, pp. 167–179, 2015.

[6] H. L. Van Trees, *Detection, Estimation, and Modulation Theory, Part I: Detection, Estimation, and Linear Modulation Theory*, 2nd ed. New York: John Wiley & Sons, 2013.

[7] S. Haykin and M. Moher, *Communication Systems*, 5th ed. New York: John Wiley & Sons, 2009.

[8] Y. Yoon, A. Kosaka, and A. C. Kak, "A new kalman-filter-based framework for fast and accurate visual tracking of rigid objects," *IEEE Transactions on Robotics*, vol. 24, no. 5, pp. 1238–1251, 2008.

[9] Y. S. Shmaliy, S. Zhao, and C. K. Ahn, "Kalman and ufir state estimation with coloured measurement noise using backward euler method," *IET Signal Processing*, vol. 14, no. 2, pp. 64–71, 2020.

[10] B. P. Gibbs, *Advanced Kalman Filtering,Least-Squares and Modeling*. New York: John Wiley & Sons, 2011.

[11] P. Liang, E. Blasch, and H. Ling, "Encoding color information for visual tracking: Algorithms and benchmark," *IEEE Transactions on Image Processing*, vol. 24, no. 12, pp. 5630–5644, 2015.

[12] A. Gelb, *Applied optimal estimation*. MIT press, 1974.

[13] M. S. Grewal and A. P. Andrews, *Kalman filtering: Theory and Practice with MATLAB*. Hoboken,NJ: John Wiley & Sons, 2014.

[14] D. Simon, *Optimal state estimation: Kalman, H_∞, and nonlinear approaches*. Hoboken,NJ: John Wiley & Sons, 2006.

[15] S. Zhao, Y. S. Shmaliy, and C. K. Ahn, "Bias-constrained optimal fusion filtering for decentralized wsn with correlated noise sources," *IEEE Transactions on Signal and Information Processing over Networks*, vol. 4, no. 4, pp. 727–735, 2018.

[16] Y. S. Shmaliy, "Linear optimal fir estimation of discrete time-invariant state-space models," *IEEE Transactions on Signal Processing*, vol. 58, no. 6, pp. 3086–3096, 2010.

[17] Y. Wu, J. Lim, and M.-H. Yang, "Online object tracking: A benchmark," in *Proceedings of the IEEE conference on computer vision and pattern recognition*, 2013, pp. 2411–2418.

[18] H. Kuhlmann, "Kalman-filtering with coloured measurement noise for deformation analysis," in *Proceedings, 11th FIG Symposium on Deformation Measurements, Santorini, Greece*, 2003.

[19] K. Wang, Y. Li, and C. Rizos, "Practical approaches to kalman filtering with time-correlated measurement errors," *IEEE Transactions on Aerospace and Electronic Systems*, vol. 48, no. 2, pp. 1669–1681, 2012.

[20] G. Chang, "On kalman filter for linear system with colored measurement noise," *Journal of Geodesy*, vol. 88, no. 12, pp. 1163–1170, 2014.

[21] Y. S. Shmaliy, S. Zhao, and C. K. Ahn, "Optimal and unbiased filtering with colored process noise using state differencing," *IEEE Signal Processing Letters*, vol. 26, no. 4, pp. 548–551, 2019.

[22] D. M. Kim and J. Suk, "GPS output signal processing considering both correlated/white measurement noise for optimal navigation filtering," *International Journal of Aeronautical and Space Sciences*, vol. 13, no. 4, pp. 499–506, 2012.

[23] J. Chen and L. Ma, "Particle filtering with correlated measurement and process noise at the same time," *IET radar, sonar & navigation*, vol. 5, no. 7, pp. 726–730, 2011.

[24] Y. S. Shmaliy, F. Lehmann, S. Zhao, and C. K. Ahn, "Comparing robustness of the kalman,h_∞, and ufir filters," *IEEE Transactions on Signal Processing*, vol. 66, no. 13, pp. 3447–3458, 2018.

[25] W. Liu, "Optimal estimation for discrete-time linear systems in the presence of multiplicative and time-correlated additive measurement noises," *IEEE Transactions on Signal Processing*, vol. 63, no. 17, pp. 4583–4593, 2015.

[26] W. Liu, P. Shi, and J.-S. Pan, "State estimation for discrete-time markov jump linear systems with time-correlated and mode-dependent measurement noise," *Automatica*, vol. 85, pp. 9–21, 2017.

[27] T. Kang, Y. Mo, D. Pae, C. Ahn, and M. Lim, "Robust visual tracking

framework in the presence of blurring by arbitrating appearance-and feature-based detection," *Measurement*, vol. 95, pp. 50–69, 2017.
[28] N. R. Gans and S. A. Hutchinson, "Stable visual servoing through hybrid switched-system control," *IEEE Transactions on Robotics*, vol. 23, no. 3, pp. 530–540, 2007.
[29] R. Verma, "A review of object detection and tracking methods," *International Journal of Advance Engineering and Research Development*, vol. 4, no. 10, pp. 569–578, 2017.
[30] A. Yilmaz, O. Javed, and M. Shah, "Object tracking: A survey," *Acm computing surveys (CSUR)*, vol. 38, no. 4, pp. 13–es, 2006.
[31] A. Bryson and D. Johansen, "Linear filtering for time-varying systems using measurements containing colored noise," *IEEE Transactions on Automatic Control*, vol. 10, no. 1, pp. 4–10, 1965.
[32] A. Bryson Jr and L. Henrikson, "Estimation using sampled data containing sequentially correlated noise," *Journal of Spacecraft and Rockets*, vol. 5, no. 6, pp. 662–665, 1968.
[33] M. G. Petovello, K. O'Keefe, G. Lachapelle, and M. E. Cannon, "Consideration of time-correlated errors in a kalman filter applicable to gnss," *Journal of Geodesy*, vol. 83, no. 1, pp. 51–56, 2009.
[34] Y. Bar-Shalom, X. R. Li, and T. Kirubarajan, *Estimation with applications to tracking and navigation: theory algorithms and software*. John Wiley & Sons, 2001.
[35] Y. S. Shmaliy, S. Zhao, and C. K. Ahn, "Unbiased finite impluse response filtering: An iterative alternative to kalman filtering ignoring noise and initial conditions," *IEEE Control Systems Magazine*, vol. 37, no. 5, pp. 70–89, 2017.
[36] Y. S. Shmaliy, "An iterative kalman-like algorithm ignoring noise and initial conditions," *IEEE Transactions on Signal Processing*, vol. 59, no. 6, pp. 2465–2473, 2011.
[37] F. Ramirez-Echeverria, A. Sarr, and Y. S. Shmaliy, "Optimal memory for discrete-time fir filters in state-space," *IEEE Transactions on Signal Processing*, vol. 62, no. 3, pp. 557–561, 2014.
[38] (2015) Datasets-visual tracker benchmark. [Online]. Available: http://www.visual-tracking.net
[39] H. Kiani Galoogahi, A. Fagg, C. Huang, D. Ramanan, and S. Lucey, "Need for speed: A benchmark for higher frame rate object tracking," in *Proceedings of the IEEE International Conference on Computer Vision*, 2017, pp. 1125–1134.
[40] B. Pueo, "High speed cameras for motion analysis in sports science," *Journal of Human Sport and Exercise*, vol. 11, no. 1, pp. 53–73, 2016.